International Journal of Geography, Geology and Environment

P-ISSN: 2706-7483
E-ISSN: 2706-7491
IJGGE 2024; 6(1): 330-346
https://www.geojournal.net
Received: 02-11-2023
Accepted: 06-12-2023

Gulista Jahan
Department of Geography, Indra Priyadarshini Govt. Girls College of Commerce Haldwani, Kumaun University, Nainital, Uttarakhand, India

Nirmala Lohani
Department of Geography, Indra Priyadarshini Govt. Girls College of Commerce Haldwani, Kumaun University, Nainital, Uttarakhand, India

Corresponding Author:
Gulista Jahan
Department of Geography, Indra Priyadarshini Govt. Girls College of Commerce Haldwani, Kumaun University, Nainital, Uttarakhand, India

Flood hazard risk zoning through AHP, GIS, and RS: A case study of Ramganaga River Basin (India)

Gulista Jahan and Nirmala Lohani

DOI: https://dx.doi.org/10.22271/27067483.2024.v6.i1e.237

Abstract
Flooding emerges as a prominent natural disaster, posing a significant global concern due to its increasing frequency, leading to elevated mortality rates and considerable economic losses. Various methods have been developed and proposed for assessing the risk of flooding. India, much like several other nations, confronts persistent challenges from annual floods, particularly in Himalayan river catchments. This study aims to harness GIS spatial analysis functions coupled with an AHP-based MCDM method, incorporating considerations from 14 different parameters spanning hydro-geomorphological, geological, climatological, physiological, and demographic aspects. The resulting output categorizes the entire basin into five distinct flooding risk zones, delineating very high, high, moderate, low, and no flooding risk. The developed flooding risk zone map highlights a substantial area, with approximately 10.2% falling under the category of very high risk and 17.8% identified as highly susceptible to flooding. The delineation of flooding zones in the current assessment of the Ramganga River basin proves advantageous for implementing effective measures in the strategic planning of flooding risk management.

Keywords: Flood hazard risk, strategic planning, flooding risk management, prominent natural disaster

Introduction
A disaster is an unforeseen and severe incident that leads to the loss of both property and lives. There are two primary categories of disasters: natural and man-made. Natural disasters encompass various types of such events such as, sudden tectonic movements resulting in earthquakes, volcanic eruptions, prolonged dry conditions leading to droughts, floods, cyclones, forest fires, cloudbursts, heat waves and more. Man-made disasters include nuclear incidents, chemical leakage, oil leakage, biological crises, fires, road accidents, terrorism, and other related events (Rosselló *et al.*, 2020; Susman *et al.*, 2019; Tierney, 2019) [33, 38, 39].
Each year, approximately 45,000 people worldwide lose their lives due to natural disasters (https://ourworldindata.org/). India, with its extensive population and geographical diversity, serves as a prominent illustration of both vulnerability and resilience in the face of such challenges. Between 1970 and 2021, over 6,000 natural and 7,000 human-made catastrophes have taken place. India, home to more than a quarter (29.02%) of the global population affected by natural disasters, has witnessed the loss of 45, 91,768 lives due to such events since 1900.
After storms, floods stand as the second most prevalent disaster (de Ruiter *et al.*, 2020; Ripple *et al.*, 2022) [5, 32]. Within India's extensive flood-prone expanse of 40 million hectares, approximately 7.5 million hectares are impacted on average each year (Kumar *et al.*, 2023; Rumpa *et al.*, 2023) [18, 34]. The Indo-Gangetic-Brahmaputra plains experience annual occurrences of floods. Flood hazards pose a significant and pressing challenge in the Indo-Gangetic plains. The analysis of floods has emerged as a critical focal point in contemporary disaster management for this region. Floods annually claim thousands of lives worldwide, underscoring the urgent need for in-depth research aimed at enhancing prediction, effective management, and timely warning procedures. Such efforts are vital to safeguard lives and mitigate the devastating impact of these recurrent natural disasters.
A disaster is the result of the collective impact of various hazards such as floods, cyclones, droughts, etc., and the vulnerabilities inherent in society, cities, or villages. The absence of either vulnerability or hazard precludes the occurrence of a disaster.

Hazard, in this context, is described as a phenomenon posing a risk to a community or system, with the potential to cause a disaster (Javadinejad *et al.*, 2019; Patel *et al.*, 2020) [9, 26]. Vulnerability, on the other hand, is characterized as the capacity of a society or system to withstand the forces of a hazard.

The extensive impact of floods in the Indian subcontinent on habitats, populations, and the economy. Recent floods have particularly affected economic and governance sectors, highlighting the need for a thorough exploration of the associated dynamics, manifestations, and consequences. This understanding is deemed crucial for formulating effective policy recommendations to tackle the challenges posed by recurring floods in the region. Various causes contribute to flooding in India, including Monsoon rains, rivers from the Himalayan region, deforestation, urbanization, poor infrastructure, climate change, glacial lake outbursts, and riverbank erosions. The primary trigger is extreme rainfall events, surpassing the land's absorption capacity and drainage systems' discharge capability, resulting in surface run-off. This water surge leads to inundation, potential debris flows, landslides, and water-borne health disasters, posing significant threats to sustainable development efforts.

GIS aids in efficient resource allocation during flood events. By overlaying data on infrastructure, population density, and critical facilities, authorities can strategically deploy resources for rescue, relief, and recovery efforts. Satellite imagery helps in post-flood damage assessment. GIS tools enable the analysis of affected areas, facilitating the planning of reconstruction and recovery efforts. GIS allows for spatial analysis, helping authorities visualize and understand the spatial relationships of various factors influencing flooding, including topography, land use, and infrastructure. High-resolution satellite imagery provides detailed maps for better visualization of flood-prone areas, aiding in decision-making and resource management.

Remote sensing and GIS technology is very smart, efficient and precise technology that does not enable in assessing and analyzing and managing the problem of flooding but also contribute in various hydro-meteorological, geological and anthropogenic problems such as landslides (Ayalew & Yamagishi, 2005; Jaafari *et al.*, 2014; Kayastha *et al.*, 2013; Keesstra *et al.*, 2012, 2013; Lee & Pradhan, 2007; Ozdemir & Altural, 2013; Pradhan *et al.*, 2010; Regmi *et al.*, 2010; Samanta *et al.*, 2018; Yalcin *et al.*, 2011; Youssef *et al.*, 2015; Singh *et al.*,2022) [2, 8, 12, 14, 13, 20, 24, 27, 31, 35, 45, 47, 36], drought susceptibility (Lakshmi *et al.*, 2020; Park *et al.*, 2017; Rahmati, Falah, *et al.*, 2020; Rahmati, *et al.*, 2020; Tirivarombo *et al.*, 2018; Tran James B.; Tran, Tri Dinh; Tran, Ha Thanh, 2017; Vicente-Serrano *et al.*, 2020; Yao *et al.*, 2018) [19, 25, 29, 30, 40, 42, 43, 46], forest fires (Freddy *et al.*, 2014; Krishna & Reddy, 2012; Prasad *et al.*, 2016; Tiwari *et al.*, 2021) [6, 15, 28, 41], earthquake vulnerability (Aghataher *et al.*, 2023; Jena *et al.*, 2021; Matin & Pradhan, 2021; Omarzadeh *et al.*, 2021; Yagoub, 2015) [1, 10, 22, 23, 44] solid waste management (De Feo & De Gisi, 2014; Hazarika & Saikia, 2020; Kapilan & Elangovan, 2018; Soltani *et al.*, 2015) [4, 7, 11, 37].

Conducting a comprehensive flood risk and vulnerability assessment for a particular region is an intricate undertaking, laden with challenges. However, leveraging the capabilities of remote sensing and Geographic Information System (GIS) alongside the Multi-criteria Decision Making Method (MCDA) not only facilitates this complex process but also empowers decision makers and planners to engage in a systematic and scientifically grounded evaluation. This integrated approach not only streamlines the assessment but also enhances the ability to address and effectively manage the multifaceted challenges associated with flood risks.

Data used in the study and sources

The study utilized two types of data: non-spatial (statistical data from census reports and various reports) and spatial (satellite images, digital elevation models, thematic maps, and digital vector data). Non-spatial data was sourced from Census of India (2011). Spatial data included Sentinel satellite images, SRTM DEM, geological and geomorphological maps from Geological Survey of India (GSI), soil maps from ICAR-NBSS & LUP, and climatic data from World Clim. Remote sensing and GIS techniques, along with ground truthing and Google Earth images, were employed for analysis. The dataset was processed using ArcGIS software. Field visits and ground control points were used for validation.

Methodological procedure of flood risk assessment

The methodology for predicting Flooding Hazard Zones in the Ramganga River Basin is depend on the very famous and reliant Multi-Criteria Decision-Making (MCDM) method that is Analytical Hierarchical Process associated with Geographic Information Systems (GIS) typically involves the following steps (Figure 1).

Identification of criteria, parameters and factors for the flood hazard zonation

On the basis of previous literature and experts' advice working in this field, the researcher identified 14 parameters from different criteria of geophysical, hydrological, climatological and anthropogenic environment. Among these parameters, some parameters are categorical and some are ratio data. The categorical data were keep in the same categories, whereas ratio data were reclassified in to the 5 classes according to Jenk's Natural Break Method in Arc GIS software.

Data collection and pre-processing

For this assessment, the geospatial data on 14 various aspects of geophysical, hydrological, climatological and anthropogenic environment of the basin was collected from various sources. These aspects were considered as parameters and factors that mainly affects the flood hazards and its vulnerability. Before taking them into account for assessment, these data was pre-processed in terms of scale, resolution, conversion from vector to raster, cleaning, reclassification resampling (re-projection to uniform coordinate system) etc. for the standardization and normalisation of the data.

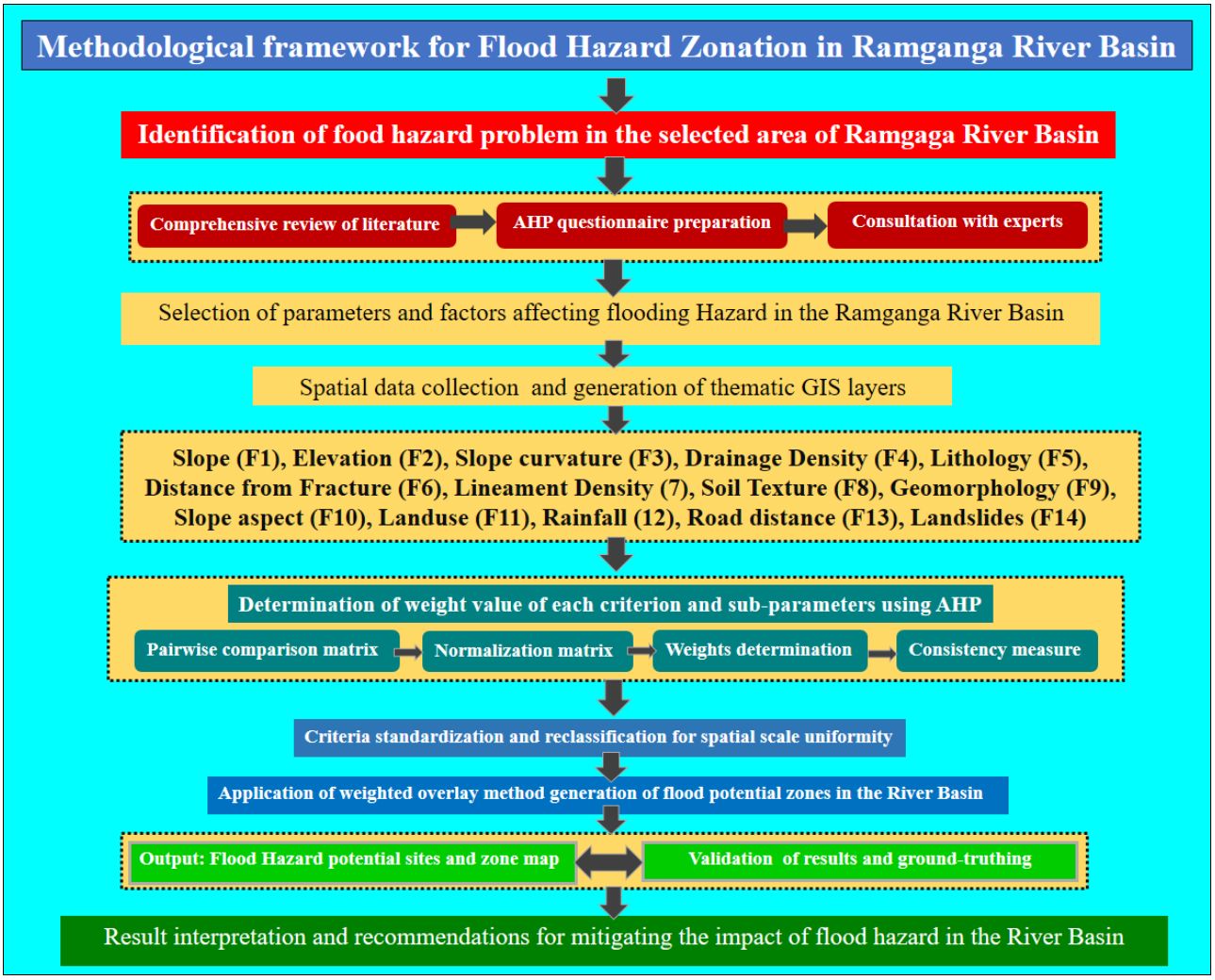

Fig 1: Methodological flowchart for the flood hazard zonation of the Ramganga river basin

Criteria weighting

In the assessment process, one of the key tasks is to determine the relative importance of the identified criteria for accurate flooding prediction, and this is achieved through criteria weighting. To accomplish this crucial step, the researcher opted for a powerful combination of Analytical Hierarchical Process (AHP) based Multi-Criteria Decision-Making Method (MCDM).

By employing the AHP in the broader MCDM approach, the researcher gains the ability to thoroughly evaluate all the criteria involved in flooding prediction. Through this comprehensive evaluation, specific weights are assigned to each parameter, reflecting their respective significance in assessing the potential flooding hazard.

The integration of AHP with MCDM empowers the researchers to make informed and well-balanced decisions when it comes to predicting and understanding the severity of flooding events. This sophisticated methodology ensures that the relative importance of each criterion is considered carefully, leading to more accurate and reliable flood predictions, ultimately contributing to improved flood risk management strategies.

Flood Hazard susceptibility mapping using Weighted Overlay Analysis

Using GIS to map the areas of high and low susceptibility to flooding hazard based on the results of the MCDM analysis. Weighted Overlay Analysis is widely used in various fields, such as urban planning, environmental management, agriculture, and disaster management. It helps stakeholders make informed decisions by considering multiple criteria simultaneously and generating a comprehensive output that accounts for the relative importance of each criterion in the decision-making process (Figure 1).

Weighted Overlay Analysis is a powerful geospatial analysis technique used in ArcGIS, a popular Geographic Information System (GIS) software. It involves combining multiple raster layers or thematic maps, each representing different criteria or factors, to generate a composite output, usually referred to as a suitability or suitability index map. For this, the researcher applied weighted sum method for this purpose. Multiply each normalized raster layer by its corresponding weight, and then sum up all the weighted layers. The result is a composite raster that represents the overall flood risk or potential of each location based on the input criteria and their assigned weights. The final composite raster was classified into different categories to represent different levels of potentiality to flood hazard. This output map provides valuable insights for decision-making processes related to flooding prone sites identification, land-use planning, flood risk reduction, mitigation and natural resource conservation and management.

Model validation and ground-truth verification

Validating the flooding prediction model by comparing the

predicted flood susceptibility with the actual flood occurrence by taking into the consideration GPS points and Google Maps. This approach offers a structured method to forecast flood susceptibility and pinpoint regions with a significant vulnerability to flooding. Its applications extend to assisting in decision-making for managing flood risks and enhancing disaster preparedness. Furthermore, it proves valuable in land-use planning and development endeavours.

Results and Discussion

Geomorphological Attributes

The geomorphology of the Ramganga River Basin, shaped by tectonic processes, erosion, and uplift, exhibits diverse landforms. The Himalayan region experiences intense erosion, contributing to the formation of dissected structural hills and valleys. The Piedmont Alluvial Plain results from the interplay of tectonic uplift, erosion, and sediment transport, forming a broad plain favorable for agriculture. Floodplains, classified as active and older, play a crucial role in river ecosystems and human systems. The river channel, a fundamental element, influences water flow, sediment transport, and flood risk. The basin's landscape features, including dams, reservoirs, ponds, lakes, and water bodies, contribute to the overall complexity (Table 2 and Figure 2). Monitoring and managing these landscapes are essential for flood risk assessment and sustainable development in the region.

Geology: Lithology and Structure

The geological composition of the Ramganga River Basin in the Himalayan region reflects complex formations shaped by tectonic processes and sedimentation over millions of years. The basin encompasses both lesser and Shiwalik Himalayan regions and an adjoining alluvial plain. The key geological features include the Himalayan frontal fault, Main Boundary fault, and various thrusts, contributing to intricate folding and faulting. The Upper Basin comprises Amora, Garhwal, and Ramgarh formations from the Proterozoic Eon, exhibiting diverse rock types. Mesoproterozoic formations (Garhwal, Jaunsar, and Ramgarh groups) consist of meta-volcanics, shale, slate, limestone, and more. Neoproterozoic formations (Baliana, Jaunsar, and Krol groups) include biamictite, quartzite, granite, and shale. Paleozoic formations (Almora and Tal groups) consist of granite, quartzite, limestone, and shale. Cretaceous formations (Sirmur and Dharamshala groups) feature massive sandy limestone. The Miocene-Pliocene period, during the Shiwalik range's evolution, exhibits sandstone and shale. The Middle to Late Pleistocene includes older alluvium deposits. The Holocene Epoch represents the latest period, featuring newer alluvium deposits (Table 2 and Figure 2). The adjacent alluvial plain is formed by sediment deposition from rivers originating in the Himalayas, primarily the Ganges and its tributaries like the Ramganga.

Table 1: Indicating geomorphological geological and soils' sub classes and nits areal attributes adopted in the flooding zonation

S.No	Landforms types	Area (Km)	Area (%)	Weights
1	Highly Dissected Structural Hills and Valleys	6160.98	19.29	1
2	Moderately Dissected Structural Hills and Valleys	592.14	1.85	1
3	Low Dissected Structural Hills and Valleys	39.97	0.13	2
4	Piedmont Slope	0.47	0.00	3
5	Piedmont Alluvial Plain	7990.91	25.02	4
6	Older Alluvial Plain	9826.73	30.77	5
7	Younger Alluvial Plain	41.29	0.13	8
8	Older Flood Plain	5376.95	16.84	9
9	Active Flood Plain	1165.29	3.65	9
10	Mass Wasting Products	7.67	0.02	4
11	Road Cutting-Anthropogenic	1.44	0.00	4
12	River	530.18	1.66	9
13	Dam and Reservoir	179.76	0.56	9
14	Pond	12.81	0.04	9
15	Waterbodies-unclassified	1.66	0.01	9
16	WatBod-Lake	6.07	0.02	9
S.N.	**Geological Formation Group**	**Area**	**Area (%)**	
1	NEWER ALLUVIUM (Meghalayan-Holocene)	8939.76	27.99	10
2	OLDER ALLUVIUM (Middle-Late Pleistocene)	16135.4	50.53	9
3	SIRMUR-Dharamshala (Palaeocene-Eocene)	17.6	0.06	8
4	SIWALIK-(Pliocene-Pleistocene)	1778.83	5.57	7
5	ALMORA-(Neoprotorozoic)	2368.64	7.42	6
6	JAUNSAR-(Neoprotorozoic)	1602.67	5.02	6
7	KROL-(Neoprotorozoic)	107.04	0.34	6
8	BALIANA-(Neoprotorozoic)	166.38	0.52	6
9	GARHWAL-(Protorozoic-Mesoprotorozoic)	541.03	1.69	5
10	RAMGARH-(Mesoproterozoic)	247.02	0.77	5
11	TAL-(Permian-Cambrian)	29.45	0.09	4
S.N.	**Soil Types**	**Area**	**Area (%)**	
1	Hills: Silty soils in on hill tops & ridges	1918.82	6.01	1
2	Hills: Loamy soils	483.14	1.51	2
3	Hills: Loamy soils in side slopes	4992.58	15.63	2
4	Hills: Loamy soils in valleys	177.73	0.56	3
5	Plains: Loamy Soils in piedmount	4530.44	14.19	3
6	Plains: Loamy Soils	1886.99	5.91	4

7	Plains: Loamy Soils in old flood plain	12283.88	38.46	5
8	Plains: Loamy Soils in New flood plain	1045.13	3.27	5
9	Plains: Silty soils in active flood plian	3049.19	9.55	5
10	Plains: Silty soils with clay in active flood plain	1569.96	4.92	5
S.N.	**LULC_NAME**	**Area**	**Area (%)**	
3	Deciduous broadleaved forest	2086.82	6.53	1
2	Closed deciduous broadleaved forest	3874.80	12.13	1
4	Deciduous needleleaved forest	1.63	0.01	1
5	Deciduous shrubland	25.03	0.08	1
6	Evergreen broadleaved forest	492.63	1.54	1
7	Evergreen needleleaved forest	2296.83	7.19	1
13	Shrubland	45.82	0.14	2
8	Grassland	21.64	0.07	2
9	Herbaceous cover	391.27	1.23	3
1	Bare areas	1.31	0.00	4
10	Built-up Land	814.31	2.55	4
11	Irrigated cropland	17836.64	55.85	5
12	Rain-fed cropland	3330.52	10.43	5
14	Tree or shrub cover (orchard)	347.93	1.09	5
15	Water body	335.91	1.05	6
16	Wetlands	31.65	0.10	6

Land use and land cover (LULC)

LULC have a profound impact on flooding in the Himalayan region and its adjacent alluvial plain. The dense forests in the Himalayan region act as natural barriers, absorbing rainwater, preventing soil erosion, and maintaining soil moisture. Deforestation can increase soil erosion and flooding. Agriculture in the alluvial plain, if not managed sustainably, can lead to soil degradation, reducing water absorption and increasing flood risk. Rapid urbanization results in impervious surfaces like concrete, reducing rainwater infiltration and increasing surface runoff, contributing to flash floods. Poorly maintained or constructed infrastructure, such as dams and embankments, can also elevate flood risks.

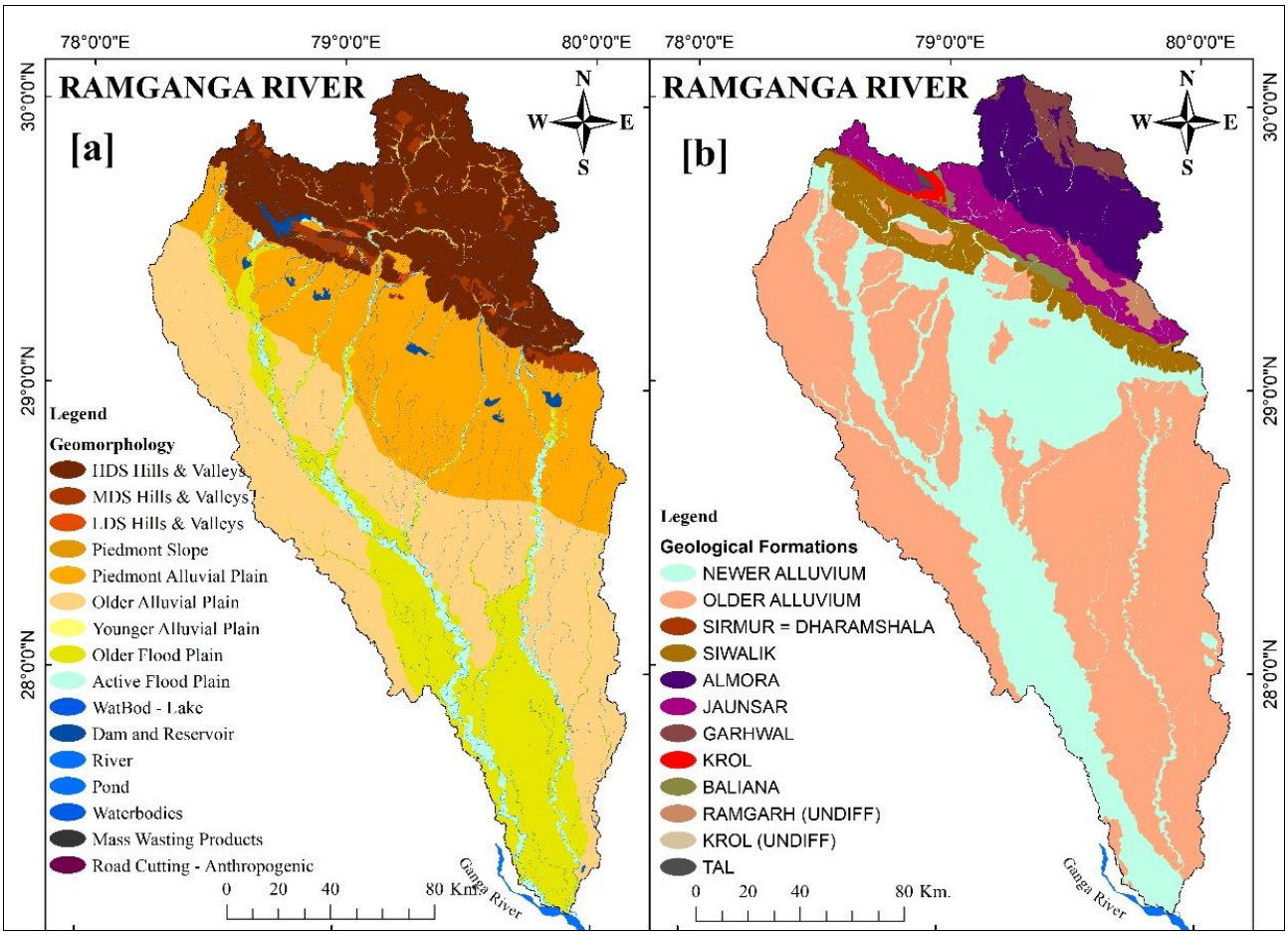

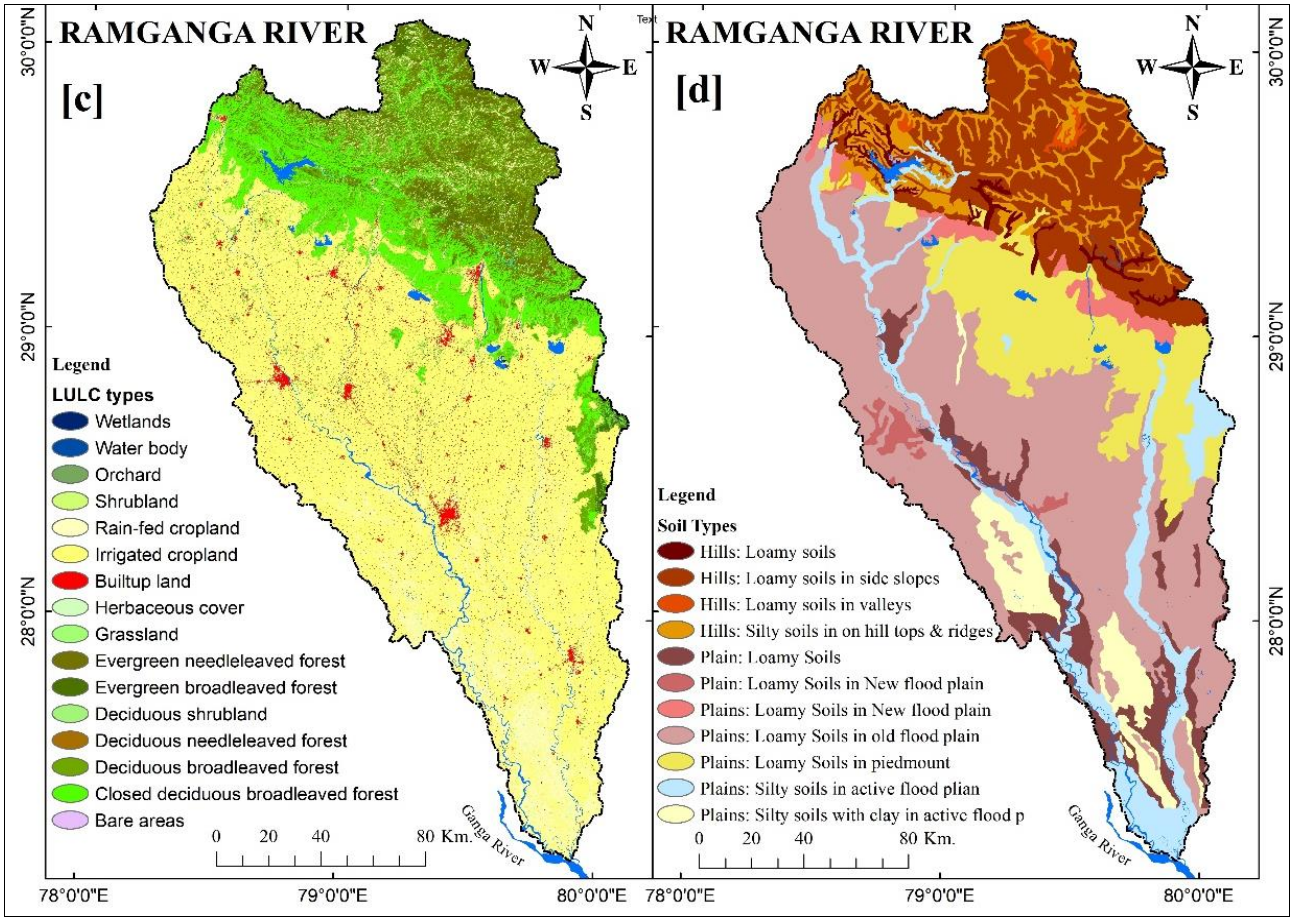

Fig 2: Maps showing (a) spatial attributes of Geomorphological landscapes, (b) Geological formations, (c) landuse landcover pattern and (d) soil properties according to major landscapes

Within the Ramganga River Basin, LULC patterns vary due to topographical differences. The northern upper segment, with diverse vegetation, is primarily forested. The southern lower region is heavily influenced by human activities, with significant areas devoted to agriculture. Forest types, including deciduous and evergreen forests, dominate the upper basin. Anthropogenic activities have transformed a substantial portion into built-up land, constituting 55.85% of the total area. Irrigated and rain-fed cropland cover 10.43%, while water bodies and wetlands occupy 1.05%. Climate change, leading to more frequent extreme weather events, can compound the impact of land-use changes in the region (Table 2 and Figure 2). In conclusion, sustaining and expanding forest cover, adopting sustainable agriculture, and appropriate infrastructure development are crucial for mitigating flood risks in the Himalayan region and its alluvial plain.

Soils

The National Bureau of Soil and Land Use Planning (NBSS & LUP) classifies soils in the Ramganga River basin into two major categories based on topographic attributes such as Hilly/Mountain Soils and Alluvial Soils of the plain. Hilly/Mountain Soils found in the high-altitude regions of the Himalayas, these soils exhibit varying proportions of silt, clay, and sand along with distinct topographic features (Table 2 and Figure 2). They are rich in organic matter and support the growth of crops like millets and pulses. However, they have low fertility, low water-holding capacity, and are prone to erosion, potentially causing landslides and stream blockages, leading to flooding.

Alluvial Soils of the plain formed through sediment deposition by rivers and streams, these soils are present in various geomorphic features in the river valleys and flood plains. Fertile and suitable for agriculture, they have a high water-holding capacity, which, during heavy rainfall, can lead to prolonged waterlogging and an increased risk of flooding. In Himalayan region and adjacent areas, the diverse soil types play a significant role in flooding, influencing water-holding capacity, erosion susceptibility, and sedimentation. Understanding these soil characteristics is essential for effective land use planning and flood management in the region.

Accessibility: Accessibility is influenced by factors like distance, travel time, and transportation mode. Access Mod 5 assesses various transportation modes—walking, cycling, public transit, and private vehicles, calculating travel times to specific destinations using each mode. This evaluation is crucial in urban, rural, and regional planning, affecting residents' quality of life and a region's economic growth. By measuring accessibility, planners can pinpoint inaccessible areas and prioritize investments in transportation infrastructure or services to enhance connectivity and accessibility for all residents. (Figure 3and Table 2)

Population distribution

Population density, measured as the number of individuals per square kilometer in an area, significantly influences the vulnerability of a region to flooding disasters. High population density often results in increased demand for land and housing, leading to urbanization and changes in

land use. This urbanization may replace natural vegetation with infrastructure, reducing the land's ability to absorb rainfall and increasing the risk of flooding. Moreover, the demand for infrastructure in densely populated areas can overwhelm drainage systems, leading to failures and flooding during heavy rainfall. High population density also complicates evacuation efforts, as limited routes may hinder safe exits during flood events (Figure 3and Table 2). Effective flood management and disaster preparedness plans must consider population density and its associated impacts on flooding severity and likelihood.

Drainage density: Drainage density, measured as the length of stream channels per unit area in a drainage basin, is a crucial factor influencing flooding. Higher drainage density, indicating more stream channels, reduces the likelihood of flooding by efficiently carrying water away and preventing surface accumulation. Conversely, lower drainage density means fewer channels, increasing the risk of flooding as water accumulates on the surface. Additionally, drainage density affects the rate of surface runoff during rainfall events. In areas with high drainage density, water is quickly carried away, reducing surface runoff and flood risk. Conversely, low drainage density leads to surface water accumulation, increasing both surface runoff and the risk of flooding (Figure 3and Table 2).

Table 2: Indicating reclassified classes and its areal attributes of the parameters adopted in the flooding zonation

S.N.	Population Density Class	Category	Area	Area %	Weights
1	89-400	Very Low	9413.2	29.48	1
2	401-800	Low	9659.9	30.26	2
3	801-1000	Moderate	8244.3	25.82	3
4	1001-1200	High	1741.7	5.46	4
5	1201-4677	Very High	2867.3	8.98	5
S.N.	**Accessibility (Minutes)**	**Accessibility Category**	**Area**	**Area (%)**	
1	0-10	Very High	9441.4	29.57	1
2	10.1-15	High	8026.9	25.14	2
3	15.1-25	Moderate	10055.6	31.49	3
4	25.1-30	Poor	2056.6	6.44	4
5	30.1-66	Very Poor	2347.4	7.35	5
S.N.	**Drainage Density**	**Category**	**Area**	**Area (%)**	
1	0-0.25	Very Coarse	9055.5	28.36	1
2	0.26-0.50	Coarse	4775.0	14.96	2
3	0.51-0.90	Moderate	10346.8	32.41	3
4	0.91-1.25	Fine	5347.0	16.75	4
5	1.251-3.66	Very Fine	2401.8	7.52	5
S.N.	**Slope Class**	**Sope Category**	**Area**	**Area (%)**	
1	< 0	Level	380.2	1.19	5
2	0.01-1.0	Genltle Slope	20237.5	63.37	3
3	1.01-3.0	Moderate	4032.0	12.63	3
4	3.01-10.0	Moderate Steep	1353.4	4.24	2
5	10.01-64.7	Steep to Very Steep	5931.3	18.57	1
S.N.	**Altitude Zone**	**Altitude Category**	**Area**	**Area (%)**	
1	125-150	Very Low	2549.3	7.98	5
2	151-200	Low	13172.9	41.25	4
3	201-250	Moderate	6478.4	20.29	3
4	251-1250	High	6136.3	19.22	2
5	1251-3100	Very High	3597.6	11.27	1
S.N.	**Curvature Index**	**Curvature Category**	**Area**	**Area (%)**	
1	-6.25-0	Plane	17472.7	54.71	2
2	0.01-0.1	Concave	10419.9	32.63	3
3	1.01-4.91	Convex	4041.8	12.66	1
S.N.	**Precipitation Class**	**Category**	**Area**	**Area (%)**	
1	879-1,200	Very Low	16246.9	50.88	1
2	1,201-1,500	Low	9436.5	29.55	2
3	1,501-1,800	Moderate	3876.4	12.14	3
4	1,801-2,100	High	2001.5	6.27	4
5	2,101-2,403	Very High	373.0	1.17	5
S.N.	**SPI Index**	**SPI Category**	**Area**	**Area (%)**	
1	4.92-6	Very Low	14255.7	44.64	5
2	6.01-8	Low	8832.6	27.66	4
3	8.01-10	Moderate	5965.9	18.68	3
4	10.1-12	High	1867.9	5.85	2
5	12.1-21.4	Very High	1012.2	3.17	1
S.N.	**TWI Index**	**SPI Category**	**Area**	**Area (%)**	
1	8.44-12	Very Low	5650.9	17.70	1
2	12.1-14	Low	15686.3	49.12	2
3	14.1-16	Moderate	6611.8	20.70	3
4	16.1-18	High	2373.1	7.43	4

5	18.1-27.9	Very High	1612.4	5.05	5
S.N.	**Flood Occrance**	**Flooding Category**	**Area**	**Area (%)**	
1	Nil	NA	31187.2	97.66	1
2	0-35	Low	141.2	0.44	2
3	36-59	Moderate	152.5	0.48	3
4	60-84	High	163.3	0.51	4
5	85-100	Very High	290.5	0.91	5

Precipitation

Precipitation plays a significant role in flooding, especially during heavy rainfall that saturates the soil and increases surface runoff. The impact of precipitation on flooding depends on factors such as rainfall intensity, duration, and existing soil moisture. Intense or prolonged rainfall can quickly saturate the soil, heightening the risk of flooding. Terrain characteristics, including steep slopes and impermeable soil, affect a region's ability to absorb rainfall and influence flooding potential. Human activities, such as urbanization, further impact precipitation effects by reducing natural land absorption, increasing surface runoff, and elevating flood risks (Figure 3 and Table 2). Understanding the dynamics of precipitation and its interaction with terrain and human factors is essential for effective flood management and disaster preparedness. This involves monitoring weather patterns, improving drainage systems, and implementing land use practices to mitigate the risk of flooding.

Surface slope

The surface slope plays a crucial role in influencing flooding in the Himalayan mountain region and its adjacent areas. Steeper slopes increase surface runoff during rainfall, leading to higher water levels in rivers and streams, and consequently, a higher risk of flooding. In contrast, flatter slopes allow easier absorption of water by the soil, reducing surface runoff and flood risk. However, flat areas also face a risk of flooding due to water accumulation. The Himalayan region exhibits varying slopes, with steep areas at higher elevations and flatter regions in valleys and plains. Understanding and considering surface slope are essential for assessing and managing flood risks, guiding the planning and design of drainage infrastructure to mitigate flooding, including the construction of canals, culverts, and retention ponds (Figure 4 and Table 2).

Surface elevation

Surface elevation is a crucial factor influencing floods in the Himalayan mountain region, foothills, and adjacent alluvial plains. Higher elevations contribute to faster water flow downhill, increasing the risk of erosion, sediment transport, and flooding. Channel capacity is affected, with narrower valleys and higher elevations making rivers more prone to flooding. Moreover, elevated areas generate more runoff due to less vegetation and thinner soils, leading to increased streamflow and downstream flooding risk. In the Himalayan mountains, higher elevations are susceptible to flash floods from intense rainfall or glacial lake outburst floods. These floods, though short-lived, can be highly destructive. In the foothills and adjacent plains, lower elevations are prone to slower-moving riverine floods from prolonged rainfall or snowmelt, covering large areas and causing extensive damage. Overall, surface elevation critically influences flood dynamics. Effective flood control in the Himalayan region requires proper land-use planning, the construction of flood control structures, and the implementation of early warning systems to mitigate flood impacts.

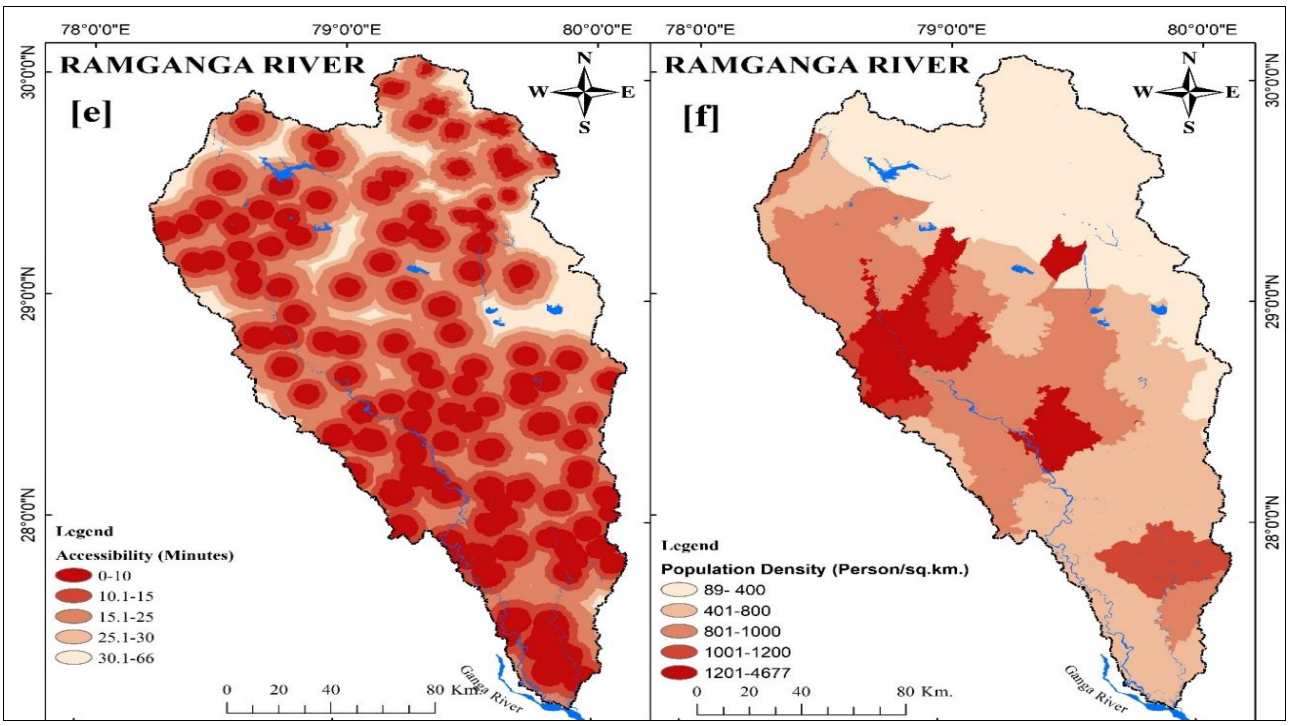

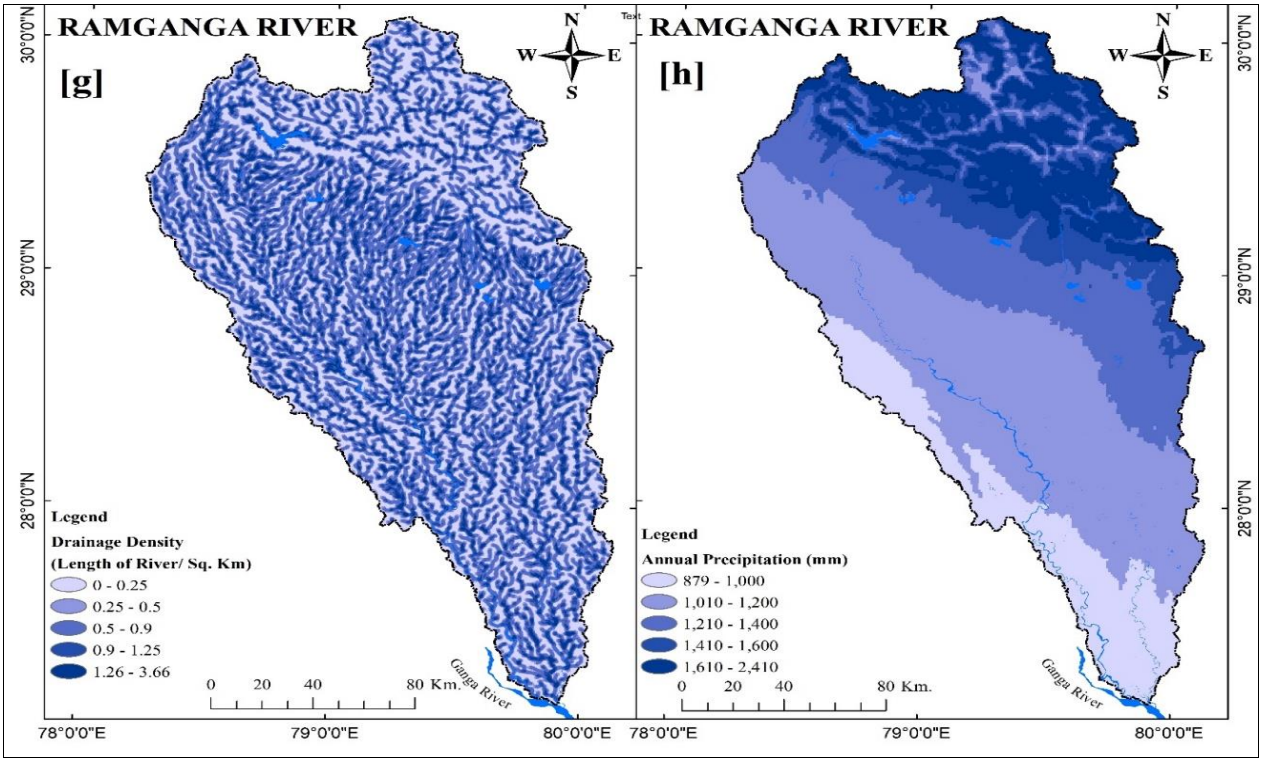

Fig 3: Showing (e) accessibility to major places, (f) population density, (g) drainage density and (h) spatial pattern of annual precipitation in the Ramganga River Basin

Planform curvature

Planform curvature (commonly called plan curvature) is perpendicular to the direction of the maximum slope. A positive value indicates the surface is sidewardly convex at that cell. A negative plan indicates the surface is sidewardly concave at that cell. A value of zero indicates the surface is linear Profile curvature relates to the convergence and divergence of flow across a surface. The curvature value can be used to find soil erosion patterns as well as the distribution of water on land. The profile curvature affects the acceleration and deceleration of flow and, therefore, influences erosion and deposition (Figure 4 and Table 2).

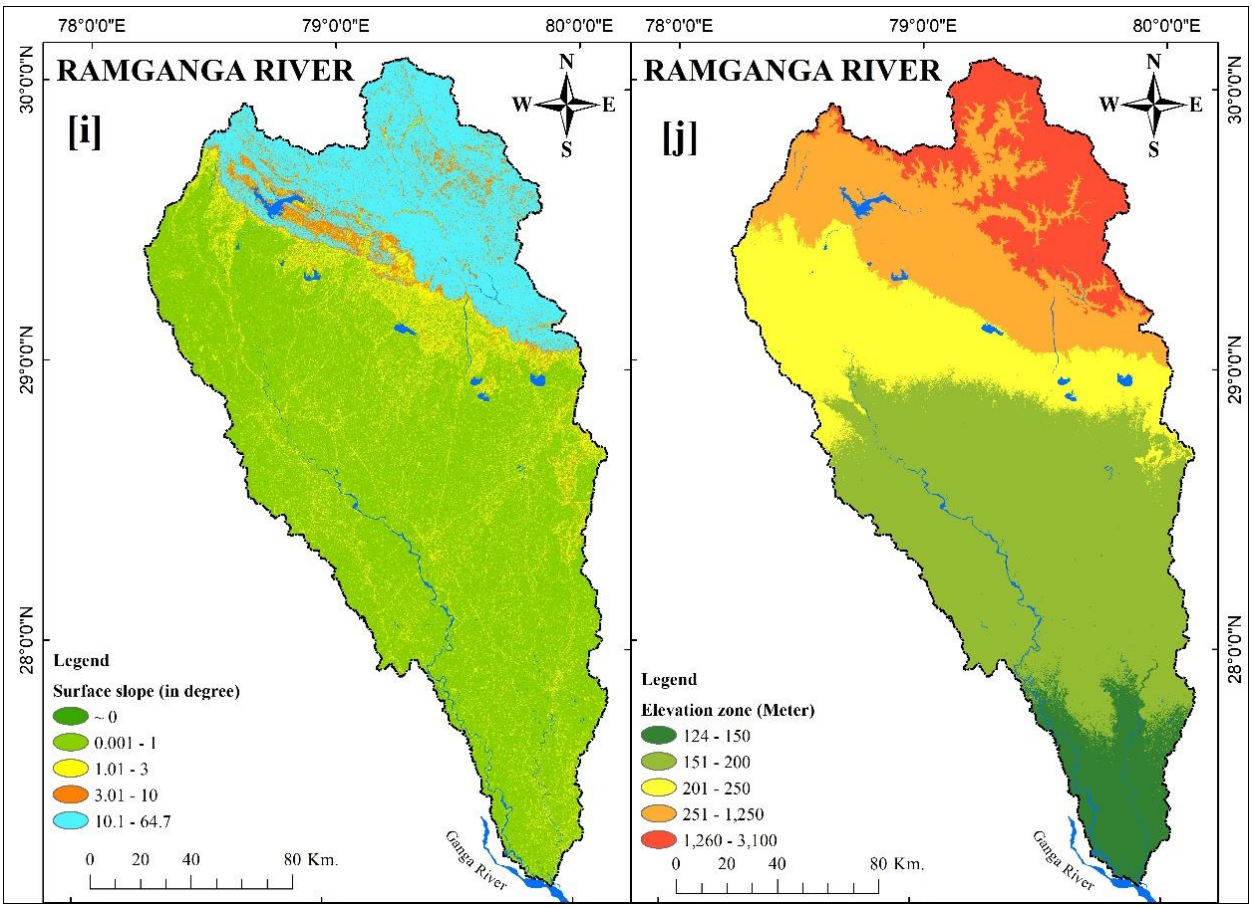

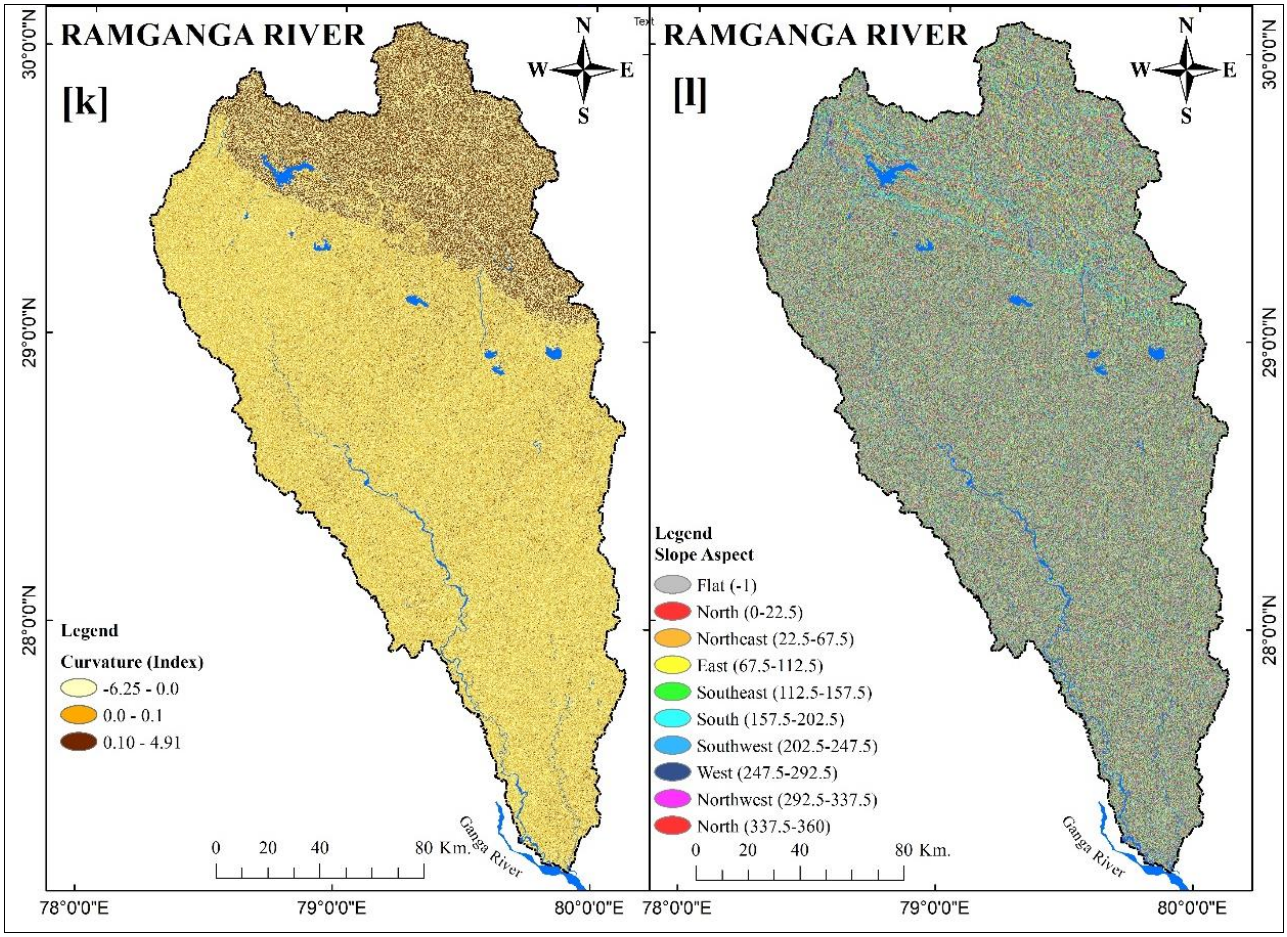

Fig 4: Showing (i) surface slope, (j) elevation extent, (k) plainform curvature of the surface and (l) slope aspect in the Ramganga River Basin

Slope Aspect

Aspect, referring to the slope's direction measured in degrees from north, significantly influences flooding dynamics. It impacts solar radiation exposure, affecting vegetation distribution, snowmelt, and soil moisture. South-facing slopes in the northern hemisphere, receiving more solar radiation, experience faster snowmelt and spring runoff, potentially raising flood risks downstream if not managed. East or west-facing slopes may undergo uneven evapotranspiration and soil moisture patterns due to varying solar radiation. Vegetation distribution on slopes is also influenced, with north-facing slopes favoring moisture-loving plants, enhancing soil infiltration. Conversely, south-facing slopes encourage drought-tolerant vegetation, increasing surface runoff. Aspect, therefore, plays a crucial role in understanding and managing flood risks associated with solar radiation and vegetation dynamics (Figure 4 and Table 2).

Slope Position Index (SPI)

The SPI is a topographic measure indicating a point's location on a slope relative to the surrounding landscape. Calculated based on slope angle and flow direction, it categorizes points as upper, middle, or lower on the slope. SPI's significance in flood management lies in its influence on water runoff. Upper slope positions, being steeper, have higher runoff potential during heavy rainfall, leading to accumulation in lower positions like valleys or floodplains. Consequently, SPI is crucial in flood risk assessment and hazard mapping, guiding the placement of flood control structures and informing land-use planning to mitigate flood risks effectively. For instance, structures may be strategically placed in lower slope positions to prevent downstream flooding, and land-use planning can avoid high-risk areas based on SPI considerations (Figure 4 and Table 2).

Topographic Wetness Index (TWI)

The TWI is a topographic measure assessing landscape wetness based on upslope contributing area and slope gradient. Ranging from 0 to infinity, higher TWI values signify wetter areas. The TWI's relevance to flooding lies in its indication of water saturation, making areas with high TWI more susceptible to surface runoff and flooding during heavy rainfall. In flood risk management, the TWI assists in identifying flood-prone areas and designing suitable measures. High TWI zones may be targeted for initiatives like wetland restoration or constructing retention ponds to manage runoff, effectively reducing flood risks. Overall, the TWI is a vital tool for flood risk assessment, providing insights into a landscape's hydrological characteristics and potential flood vulnerabilities (Figure 4 and Table 2).

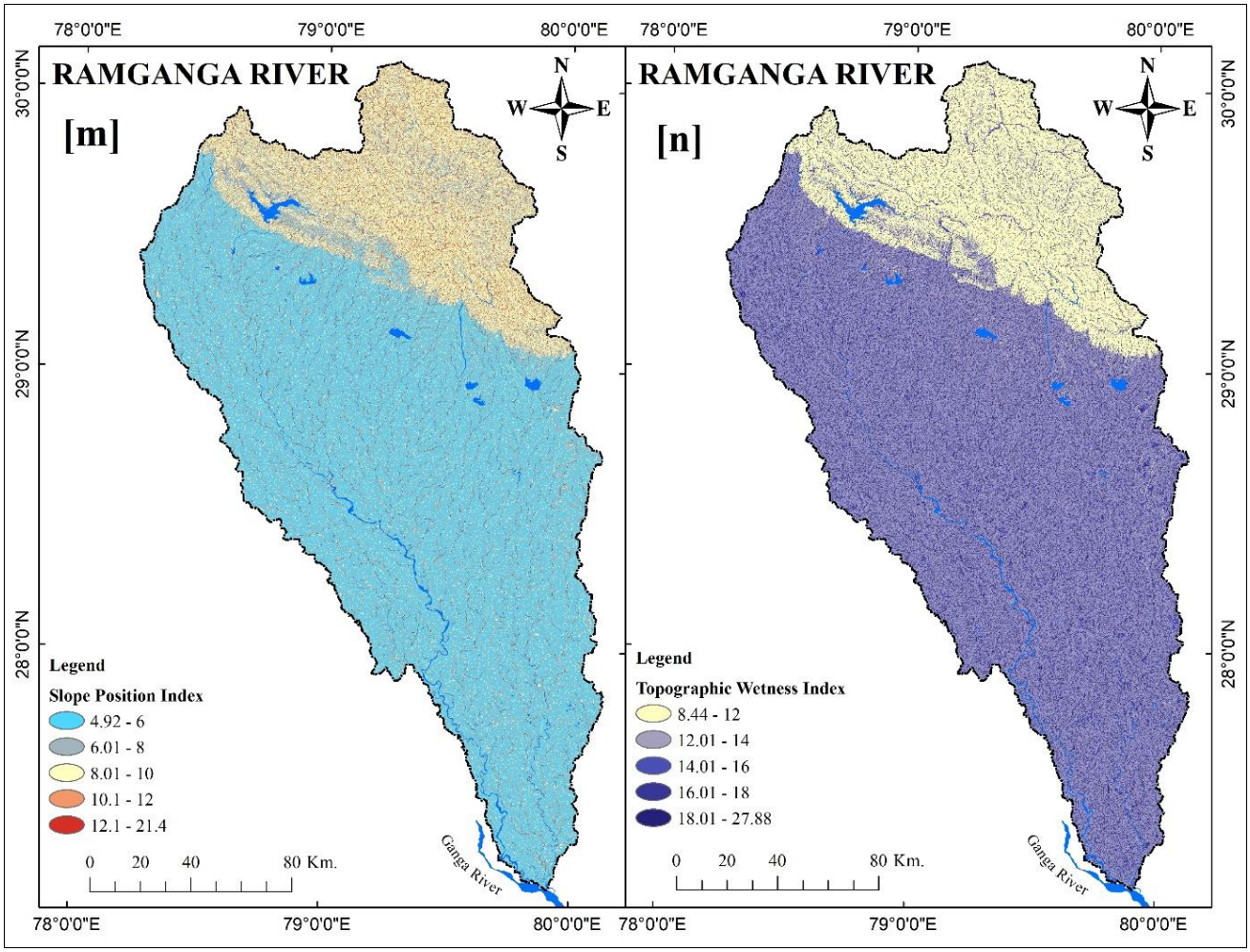

Fig 5: Showing (m) Slope Position Index (SPI) and (n) Topographic Wetness Index (TWI) of the Ramganga River Basin

Application of Multi-criteria Decision Making Method (MCDM): Analytical Hierarchical Process

Numerous research articles, reports and publications pertaining to flood hazard mapping employing the Analytic Hierarchy Process (AHP) are reviewed and summarized individually. These works are summarized with a focus on the flood-affecting parameters that were considered and the corresponding weightages assigned within the AHP framework. The following sections provide summaries of these articles.

Step I-Identify the decision problem: For the determine the flooding hazard risk sites in the river basin, there has been various criteria and alternatives identified and generated in the form of spatial layers given in the table 1.

Step II-Create a hierarchy: All the determined criteria and alternatives were organized into a hierarchical structure shown in table 1. The top level of the hierarchy is the goal or objective of the decision, the next level is the criteria and the lowest level are the alternatives.

Step III-Pairwise comparisons: To compare each criterion with every other criterion and assigned a relative importance score. The scale suggested by Saaty (1980) of 1 to 9, where 1 represents equal importance and 9 represents extreme importance (Table 3,4).and the random inconsistency indices (RI) for N=12 is shown in Table 5.

For a pair-wise comparison matrix (normalization)

$$\begin{Bmatrix} C11 & C12 & C13 \\ C21 & C22 & C23 \\ C31 & C32 & C33 \\ \ddots & \ddots & \ddots \end{Bmatrix}$$ (Table 6)

In step 1, column-wise summation values estimated for the pair-wise comparison matrix (Table 6).

$$[Cij = \sum_{i}^{n} = 1Cij]$$ (Equation 1)

In step 2, divide each component in the column-wise matrix to generate a synthesized matrix (normalized pair-wise comparison matrix)

$$\left[Cij = \frac{Cij}{\sum_{i}^{n}=1Cij}\right]$$ (Equation 2)

$$\begin{Bmatrix} X11 & X12 & X13 \\ X21 & X22 & X23 \\ X31 & X32 & X33 \\ \ddots & \ddots & \ddots \end{Bmatrix}$$ (Table 7)

Step IV-Calculate weights: The pairwise comparison scores were used to calculate the weights for each criterion. This was done by averaging the scores for each criterion and

normalizing them so that they add up to 1 (Table 7).
In step 3, divide the sum of synthesized matrix values by the criteria number used (n) to establish a weighted matrix (priority vector),

$$\left[Wij = \frac{\sum_{i}^{n=1} Xij}{n}\right] \quad \text{(Equation 3)}$$

$$\begin{Bmatrix} X13 \\ X23 \\ X33 \\ \vdots \end{Bmatrix} \quad \text{(Table 7)}$$

Step V-Consistency analysis: To check the consistency of the pairwise comparison scores the consistency ratio (CR) was taken into account. The CR measures the degree of consistency in the comparison matrix and should be less than or equal to 0.1 for the comparison matrix to be considered consistent. If the CR is greater than 0.1, revise the pairwise comparisons until a consistent comparison matrix is obtained (Saaty, 1980).
The consistency analysis: Consistency vector is computed by multiplying the pairwise matrix with the vector weights,

$$\begin{Bmatrix} C11 & C12 & C13 \\ C21 & C22 & C23 \\ C31 & C32 & C33 \\ \ddots & \ddots & \ddots \end{Bmatrix} * \begin{Bmatrix} W13 \\ W23 \\ W33 \\ \vdots \end{Bmatrix} = \begin{Bmatrix} cv13 \\ cv23 \\ cv33 \\ \vdots \end{Bmatrix} \quad \text{(Table 7)}$$

Then it is adept by separating the criterion weight and weighted sum vector

$$Cv_{11} = \frac{1}{W11}\,[C_{11}W_{11} + C_{12}W_{21} + C_{13}W_{31}]$$

$$Cv_{21} = \frac{1}{W21}\,[C_{21}W_{11} + C_{22}W_{21} + C_{23}W_{31}]$$

$$Cv_{31} = \frac{1}{W31}\,[C_{31}W_{11} + C_{32}W_{21} + C_{33}W_{31}]$$

λ_{Max} is estimated by mean value of the Consistency Vector

$$\left[\lambda max = \sum_{i-1}^{n} = CVij\right] \quad \text{(Equation 4)}$$

CI measures the deviation,

$$\left[CI = \frac{\lambda - 1}{n - 1}\right] \quad \text{(Equation 5)}$$

Where n denotes the criteria used for the analysis (Table 7)

$$\left[Cr = \frac{CI}{RI}\right] \quad \text{(Equation 6)}$$

Following the aforementioned process, the maximum eigenvalue (λ), calculated using equation (4), was determined to be 12.70 for 12 parameters and Table 7 also displays the maximum eigenvalue (λ) of each sub-criteria that was evaluated separately. A consistency index (CI) of 0.06 was discovered using Equation-(5) calculations. For the 12 number parameters and the sub-criteria in (Table 7), the random index (RI) has already been assigned a value of 1.48 (Table 5).
Later, consistency ratio (CR) values for all the sub-parameters were calculated using Equation-(6) and found to be 0.04 for the major criterion. According to Saaty (1980), the consistency degree is satisfactory if CR is less than 0.10. Because of this, the AHP model might not produce statistically significant results if it is more than 0.10, which suggests irregularities in the evaluation process. All of the CR values for the sub-parameters are less than 0.10, as shown in Table 7. This establishes the consistency of the preferences used to create the comparison matrices.

Table 3: The preference scale for pair wise comparison in AHP Scale

Scale	Degree of preference	Explanation
1	Two criteria accord equal importance	Two activities lead to the objectives
3	Moderate significance of one aspect to another	Judgments and experience slightly indulge one action to another
5	Strong or essential importance of one parameter over another	Experience and judgments strongly favor one action over another
7	Very strong significance of one parameter over another	An activity is chosen strongly over another, dominance is established in practice
9	Extreme significance of one factor over another	The indication preferring one action over another is of highest probable order of assertion
2,4,6,8	Intermediate values within two nearby judgments	When conciliation is required
Reciprocals	Opposites	Used for inverse comparison

Source: Adopted from Saaty, T.L. 1980

Table 4: Matrix for the pair-wise comparison for multi-criteria decision-making (MCDM) method

S.N.	**Main Criteria**	**F1**	**F2**	**F3**	**F4**	**F5**	**F6**	**F7**	**F8**	**F9**	**F10**	**F11**	**F12**	**F13**	**F14**
1	Slope (F1)	1	2	2	3	4	5	6	6	6	7	8	8	8	9
2	Elevation (F2)	1/2	1	2	3	4	4	5	5	5	6	7	7	8	9
3	Slope curvature (F3)	1/2	1/2	1	2	3	4	5	6	7	7	8	8	8	9
4	Drainage Density (F4)	1/3	1/3	1/2	1	2	3	4	5	5	6	6	7	8	9
5	Lithology (F5)	1/4	1/4	1/3	1/2	1	2	3	4	4	5	6	7	8	9
6	Distance from Fracture (F6)	1/5	1/4	1/4	1/3	1/2	1	2	3	3	4	5	6	7	8
7	Lineament Density (7)	1/6	1/5	1/5	1/4	1/3	1/2	1	2	2	3	4	5	6	7
8	Soil Texture (F8)	1/6	1/5	1/6	1/5	1/4	1/3	1/2	1	1	2	3	4	5	6

9	Geomorphology (F9)	1/6	1/5	1/7	1/5	1/4	1/3	1/2	1	1	2	3	4	5	6
10	Slope aspect (F10)	1/7	1/6	1/7	1/6	1/5	1/4	1/3	1/2	1/2	1	2	3	4	5
11	Landuse landcover (F11)	1/8	1/7	1/8	1/6	1/6	1/5	1/4	1/3	1/3	1/2	1	2	3	4
12	Rainfall (12)	1/8	1/7	1/8	1/7	1/7	1/6	1/5	1/4	1/4	1/3	1/2	1	2	3
13	Road distance (F13)	1/8	1/8	1/8	1/8	1/8	1/7	1/7	1/5	1/5	1/4	1/3	1/2	1	2
14	Landslides (F14)	1/9	1/9	1/9	1/9	1/9	1/8	1/7	1/6	1/6	1/5	1/4	1/3	1/2	1

Table 5: Synthesized matrix for MCDM method

Criteria	C1	C2	C3	C4	C5	C6	C7	C8	C9	C10	C11	C12	C13	C14	Weights	λ Max
F1	0.26	0.36	0.28	0.27	0.25	0.24	0.21	0.17	0.17	0.16	0.15	0.13	0.11	0.10	0.20	0.80
F2	0.13	0.18	0.28	0.27	0.25	0.19	0.18	0.15	0.14	0.14	0.13	0.11	0.11	0.10	0.17	0.94
F3	0.13	0.09	0.14	0.18	0.19	0.19	0.18	0.17	0.20	0.16	0.15	0.13	0.11	0.10	0.15	1.09
F4	0.09	0.06	0.07	0.09	0.12	0.14	0.14	0.15	0.14	0.14	0.11	0.11	0.11	0.10	0.11	1.25
F5	0.06	0.04	0.05	0.04	0.06	0.10	0.11	0.12	0.11	0.11	0.11	0.11	0.11	0.10	0.09	1.42
F6	0.05	0.04	0.03	0.03	0.03	0.05	0.07	0.09	0.08	0.09	0.09	0.10	0.10	0.09	0.07	1.42
F7	0.04	0.04	0.03	0.02	0.02	0.02	0.04	0.06	0.06	0.07	0.07	0.08	0.08	0.08	0.05	1.42
F8	0.04	0.04	0.02	0.02	0.02	0.02	0.02	0.03	0.03	0.05	0.06	0.06	0.07	0.07	0.04	1.30
F9	0.04	0.04	0.02	0.02	0.02	0.02	0.02	0.03	0.03	0.05	0.06	0.06	0.07	0.07	0.04	1.33
F10	0.04	0.03	0.02	0.01	0.01	0.01	0.01	0.01	0.01	0.02	0.04	0.05	0.05	0.06	0.03	1.22
F11	0.03	0.03	0.02	0.01	0.01	0.01	0.01	0.01	0.01	0.01	0.02	0.03	0.04	0.05	0.02	1.10
F12	0.03	0.03	0.02	0.01	0.01	0.01	0.01	0.01	0.01	0.01	0.01	0.02	0.03	0.03	0.02	0.99
F13	0.03	0.02	0.02	0.01	0.01	0.01	0.01	0.01	0.01	0.01	0.01	0.01	0.01	0.02	0.01	0.89
F14	0.03	0.02	0.02	0.01	0.01	0.01	0.01	0.00	0.00	0.00	0.00	0.01	0.01	0.01	0.01	0.83
																16.00

Table 6: Random Inconsistency (RI) indices for n= 10

N	1	2	3	4	5	6	7	8	9	10
RI	0.00	0.00	0.58	0.90	1.12	1.24	1.32	1.41	1.46	1.49

Suitability Index (SI) values were calculated using various methods, such as the weighted linear combination (WLC) method, the analytical hierarchy process (AHP) method (Malczewski, 1999). These methods use different mathematical algorithms to combine the weighted criteria and produce the suitability index values. Finally, the techniques overlay individual criteria layers to produce a composite suitability map.

A dimensionless number known as the Suitability Index (SI) is related to the mapping of potential flooding sites in the basin. The final layer was generated and once further classified into five appropriate zones of flooding hazard risk suitability after weighted overlay analysis in Arc GIS Modular was applied. The following equation was used to calculate each land's final potential for flooring risk score;

$$LSI = \sum_i^n W_i X_i \quad \text{(Equation 7)}$$

Where 'W_i' denotes the multiplication of all associated weights in the hierarchy of 'i^{th}' factors offered for a specific class of the 'i^{th}' factor found on the assessed land unit, and "LSI" stands for "land suitability index." Table 8 shows an assessment of the overall suitability score. The following equation was used to assess final suitability index for potential flooding sites in the region:

$$LSI = \sum_i^n (sl_x sl_y + Elv_x Elv_y + Cs_x Cs_y + Dd_x Dd_y + Lth_x Lth_y + Dfr_x Dfr_y + Ld_x Ld_y + St_x St_y + Gm_x Gm_y + Sa_x Sa_y + LULC_x LULC_y + Rf_x Rf_y + Rd_x Rd_y + Ls_x Ls_y)$$

(Equation 8)

Where, Slope (Sl), Elevation (Elv), Slope curvature (Sc), Drainage Density (Dd), Lithology (Lth), Distance from Fracture (Dfr), Lineament Density (Ld), Soil Texture (St), Geomorphology (Gm), Slope aspect (Sa), Landuse landcover (LULC), Rainfall (Rf), Road distance (Rd), Landslides (Ls) and subscripts, i.e. 'x' designate normalized weight of theme found through AHP. Subscripts 'y' indicates the normalized weight of the individual feature class of a theme. In MCE using a weighted linear combination, the assigned weights require to be summed up to 1 for each subcategory and category.

The suitability index values can be defined on a scale of 0 to 1 or 0 to 100, where 0 represents unsuitable locations, and 1 or 100 represents the most suitable locations. The suitability index values were classified into different categories, such as No flood, low, moderate, high and very high risk of flooding, to facilitate decision-making. This scheme of classification was adopted by many studies (Gigović, *et al.*, 2016; Çetinkaya, *et al.*, 2018, Chaudhary *et al.*, 2021; Kumar *et al.*, 2021, 2022) pertain to flooding Hazard risk assessment. The total risk index value is estimated by multiplying the score of criteria values by adding all the weighted results (Table 8).

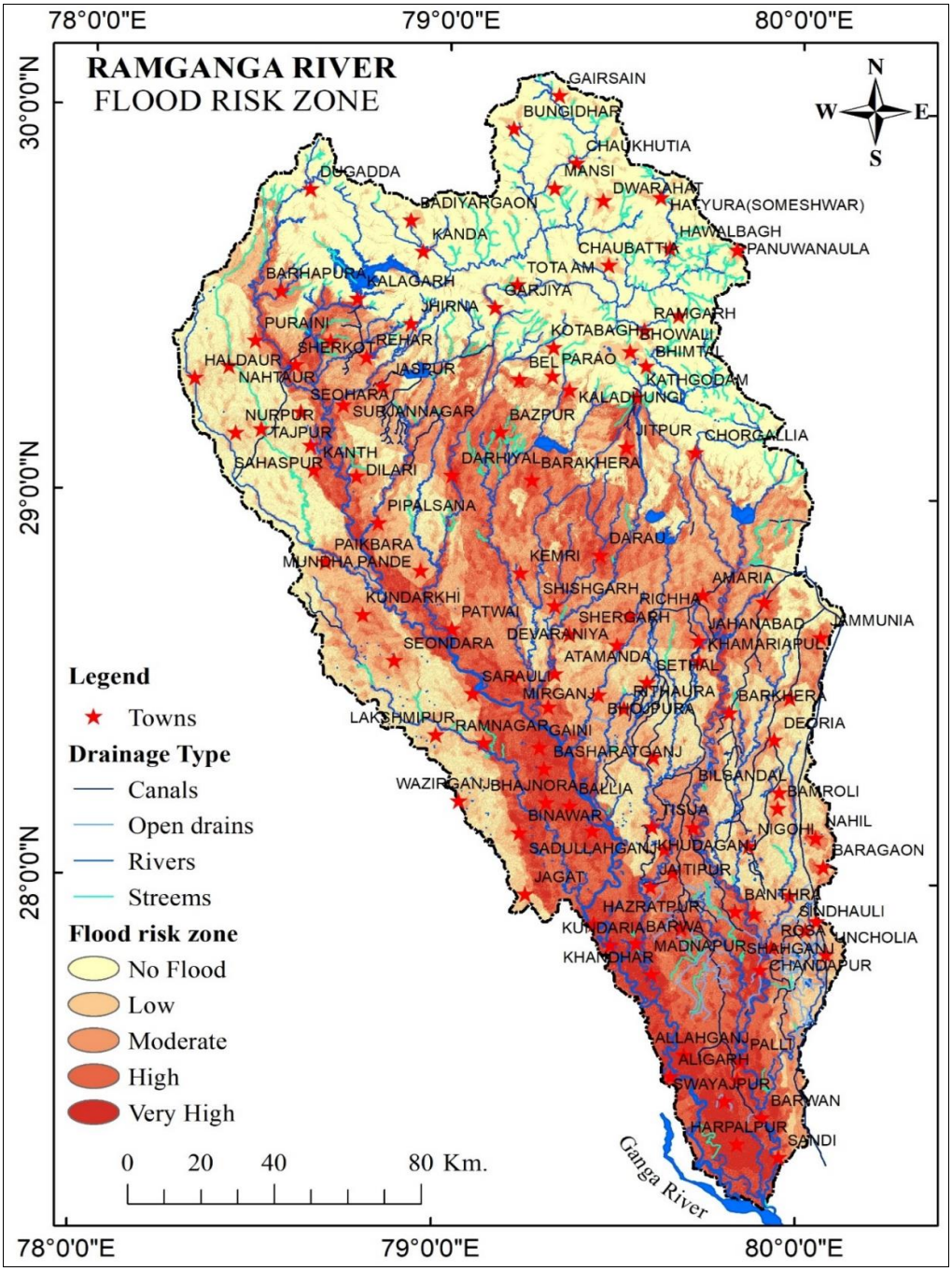

Fig 6: Showing flood risk zone in Ramganga River Basin

Table 7: district-wise areal distribution in different flooding hazard risk zones in the Ramganga River Basin

Districts	Flooding risk categories and areal coverage in square km and in percentage										
	Very High		High		Moderate		Low		Very Low		Total Area
	sq. km	%	sq. km	%	sq. km	%	sq. km	%	sq. km	%	sq. km
Almora	2.3	0.1	6.8	0.3	62.6	2.4	368.7	14.4	2127.2	82.8	2567.6
Budaun	277.2	22.5	367.8	29.8	139.2	11.3	289.6	23.5	444.2	13.0	1518.0
Bareilly	567.0	13.8	857.8	20.8	1092.7	26.5	1179.9	28.6	423.8	10.3	4121.2
Bijnor	144.8	5.4	341.0	12.8	506.6	19.0	763.5	28.6	915.8	34.3	2671.7
Chamoli	0.0	0.0	0.1	0.0	4.7	1.5	36.1	11.2	282.1	87.3	323.0
Champawat	0.2	0.4	0.6	1.1	1.2	2.3	4.2	8.1	45.4	88.1	51.5
Hardoi	671.5	40.5	568.4	34.3	233.8	14.1	155.8	9.4	26.7	1.6	1656.3
JP nagar	20.5	3.7	51.0	9.3	37.1	6.8	129.8	23.8	307.7	56.3	546.1
Moradabad	196.4	8.7	331.2	14.7	694.3	30.9	774.4	34.4	254.0	11.3	2250.3
Nanital	76.7	2.0	266.5	6.9	323.3	8.4	787.3	20.4	2413.8	62.4	3867.6
Pauri garhwal	33.5	1.7	40.7	2.1	78.6	4.0	224.7	11.4	1599.0	80.9	1976.5
Pilhibhit	92.5	3.9	346.1	14.7	750.1	31.9	732.1	31.1	430.1	18.3	2351.0
Rampur	251.8	10.6	775.4	32.8	749.7	31.7	385.6	16.3	204.2	8.6	2366.7
Shahjahanpur	715.8	22.7	978.2	31.0	638.5	20.2	566.1	18.0	255.0	8.1	3153.6
US nagar	168.7	6.7	709.8	28.2	855.3	34.0	466.1	18.5	313.6	12.5	2513.4
Total	3218.9	10.1	5641.3	17.7	6167.8	19.3	6864.0	21.5	10042.5	31.4	31934.5

Results and Discussion

The flood Hazard risk map generated using weighted overlay analysis model results shows that 10.2% area of the Ramganga River Basin is very highly prone area (Fig. 8). These are the areas inundated for the majority of monsoon seasons by catastrophic floods. Analysis of flood-affected areas by the districts of Uttar Pradesh and Uttarakhand shows that more all less all divisions are prone to flooding. The study determined that the Bareilley, Budaun, Shahjahanpur and Hardoi districts are the most extremely high flood-prone area, accounting for 40.5% out of 5.2% of the area recognised out of total area of Ramganga River Basin. A significantly lower portion of the Ramganga Basin extremely highly prone zone was due to there being less direct influence from primary river flow originating in the mountains. From the different levels of suitability, it is possible to identify appropriate places for rehabilitation during the flooding. The suitability ranking was done under the category of very highly, highly, moderately, low, Not Suitable (No flooding zone) under flooding risk, as shown in Fig. 9. The identified suitability map estimates that the very highly suitable for flooding risk was 10.2% area, the highly suitable area was 17.8%, the moderate suitable area was 19.4%, the low suitability area was 21.7% and 30.6% area implies in the no flooding zone or not suitable for flooding. Besides the flooding risk suitable zones, around 1.15% of the area was confined in perennial waterbodies and wetlands. Analysis of the flooded areas indicates that the areas in upper part (Bijnor, Moradabad and Rampur) and the lower parts (Bareilly, Shahnjahanur and Hardoi) of the river basin experiences more floods almost every year (Table 7). Out of all the 15 districts, 9 districts are mainly affected due to flooding in the basin.

The plain of River Ganga and the plain of its sub-tributaries like Ramganaga River is one of the most frequent flood disasters affected region of the Country, and it is under constant threat of flooding, which damages infrastructure, lives, considerable number of foods causes substantial financial losses. The flood inundation extent, flood hazard risk map is beneficial for the disaster management authorities in terms of supporting the preparation, relief and rescue operations in the region. The study's findings are appropriate for resource allocation decisions in rural planning for disaster management. Using the long-term flood extents and other factors, flood hazard risk zonation maps were produced for establishing safe flood evacuation sites. Since this region is a piedmont of the Himalayas and catchment of various rivers, it is challenging to avoid floods without the intervention of flood control work. Usually, the regular flood inundation areas strongly correlate with the locations and flood control activities.

Among the different kinds of flood prevention initiations, the provision of emergency safe shelters is considered the best flood management approach as it does not cause any negative consequences on water flow and environmental conditions. Nevertheless, these safe shelters must be built on locations of maximum efficiency for safer relocation. Shelters built far from settlements or on inaccessible sites are not helpful for mitigation. The worry of flood disaster management is establishing shelters in suitable locations, but this is ignored in these areas of India as sometimes flood shelters are constructed on sites close to influential elite villagers. In addition, sometimes, the state government has attempted to turn a school into a flood shelter in some places along the rivers. In this case, remote sensing and GIS technology can play a vital role in addressing those issues and identifying locations based on unbiased scientific analysis. In this regard, findings of this study, which can visualise the sites with the most potential for flooding risk. Flood hazard zonation is also an essential step for future flood disaster management. The probability that a flood of a certain intensity will occur over an extended period is determined. Flood hazard is mainly used to define flood-prone zones. There are vast populations in the vicinity of this river basin affected by flood disasters because flood hazard areas are not demarcated using GIS and remote sensing approaches. The flood hazard map can strongly discourage people from establishing their houses in flood-prone areas. In the past, several flood mapping investigation was conducted for flood mapping to assist relief works. After that, few flood inundation mapping studies have been undertaken mainly through theoretical researchers related to flood in this region without focusing on emergency response and post-flood disaster management identifying flood hazard risk. However, real-time flood map performs a vital role in relief operations. Also, long term flood inundation maps play a crucial role in planning, decision-making and executing flood management work.

References

1. Aghataher R, Rabieifar H, Samany NN, Rezayan H. The suitability mapping of an urban spatial structure for earthquake disaster response using a gradient rain optimization algorithm (GROA). Heliyon. 2023 Oct;9(10):e20525. Available from: https://doi.org/10.1016/j.heliyon.2023.e20525
2. Ayalew L, Yamagishi H. The application of GIS-based logistic regression for landslide susceptibility mapping in the Kakuda-Yahiko Mountains, Central Japan. Geomorphology; c2005 [cited 2024 Mar]. Available from: https://doi.org/10.1016/j.geomorph.2004.06.010
3. Chaudhary S, Kumar A, Pramanik M, Negi MS. Land evaluation and sustainable development of ecotourism in the Garhwal Himalayan region using geospatial technology and analytical hierarchy process. Environ Dev Sustain; c2021 [cited 2024 Mar]. Available from: https://doi.org/10.1007/s10668-021-01528-4
4. Feo DG, Gisi DS. Using MCDA and GIS for hazardous waste landfill siting considering land scarcity for waste disposal. Waste Manag. 2014 [Cited 2024 Mar];34(11):2225-38.
5. Ruiter D MC, Couasnon A, Homberg VDMJC, Daniell JE, Gill JC, Ward PJ. Why we can no longer ignore consecutive disasters. Earth's Future. 2020 [Cited 2024 Mar];8(3):e2019EF001425.
6. Freddy AJ, Tennyson S, Samraj DA, Roy A. Detection using remote sensing and geographical information system in Pathri Reserve Forest, Uttarakhand, India; c2014. p. 353-65.
7. Hazarika R, Saikia A. Landfill site suitability analysis using AHP for solid waste management in the Guwahati Metropolitan Area, India. Arab J Geosci. 2020 [Cited 2024 Mar];13:1-14.
8. Jaafari A, Najafi A, Keesstra S, Pourghasemi HR, Rezaeian J, Sattarian A, *et al.* GIS-based frequency ratio and index of entropy models for landslide susceptibility assessment in the Caspian forest, northern Iran. Int J Environ Sci Technol. 2014 [Cited 2024 Mar].

Available from: https://doi.org/10.1007/s13762-013-0464-0
9. Javadinejad S, Eslamian S, Askari OAK, Nekooei M, Azam N, Talebmorad H, *et al.* Relationship between climate change, natural disaster, and resilience in rural and urban societies. In: Handbook of Climate Change Resilience; c2019. p. 1-25.
10. Jena R, Pradhan B, Beydoun G, Alamri A, Shanableh A. Spatial earthquake vulnerability assessment by using multi-criteria decision making and probabilistic neural network techniques in Odisha, India. Geocarto Int. 2021 [Cited 2024 Mar]. Available from: https://doi.org/10.1080/10106049.2021.1992023
11. Kapilan S, Elangovan K. Potential landfill site selection for solid waste disposal using GIS and multi-criteria decision analysis (MCDA). J Cent South Univ. 2018;25(3):570-85.
12. Kayastha P, Dhital MR, De Smedt F. Application of the analytical hierarchy process (AHP) for landslide susceptibility mapping: A case study from the Tinau watershed, west Nepal. Comput Geosci. 2013;52:398-408. Available from: https://doi.org/10.1016/j.cageo.2012.11.003
13. Keesstra S, Keesstra S, Pourghasemi HR, Pourghasemi HR, Pradhan B, Pradhan B, *et al.* Application of weights-of-evidence and certainty factor models and their comparison in landslide susceptibility mapping at Haraz watershed, Iran. Arab J Geosci. 2013. Available from: https://doi.org/10.1007/s12517-012-0532-7
14. Keesstra S, Pourghasemi HR, Pradhan B, Gokceoglu C. Application of fuzzy logic and analytical hierarchy process (AHP) to landslide susceptibility mapping at Haraz watershed, Iran. Nat Hazards. 2012. Available from: https://doi.org/10.1007/s11069-012-0217-2
15. Krishna PH, Reddy CS. Assessment of increasing threat of forest fires in Rajasthan, India using multi-temporal remote sensing data (2005-2010). 2012;(9).
16. Kumar A, Pramanik M, Chaudhary S, Negi MS. Land evaluation for sustainable development of Himalayan agriculture using RS-GIS in conjunction with analytic hierarchy process and frequency ratio. J Saudi Soc Agric Sci. 2021;20(1):1-17. Available from: https://doi.org/10.1016/j.jssas.2020.10.001
17. Kumar A, Pramanik M, Chaudhary S, Negi MS, Szabo S. Geospatial multi-criteria evaluation to identify groundwater potential in a Himalayan District, Rudraprayag, India. In: Environment, Development and Sustainability. Springer Netherlands; 2022. Available from: https://doi.org/10.1007/s10668-021-02107-3
18. Kumar R, Kumar M, Tiwari A, Majid SI, Bhadwal S, Sahu N, *et al.* Assessment and Mapping of Riverine Flood Susceptibility (RFS) in India through Coupled Multicriteria Decision Making Models and Geospatial Techniques. Water. 2023;15(22):3918.
19. Lakshmi SV, Ramalakshmi M, Rakshith RK, Christobel MJ, Kumar PP, Priyadharshini B, *et al.* An integration of geospatial technology and standard precipitation index (SPI) for drought vulnerability assessment for a part of Namakkal district, South India. Mater Today: Proc. 2020;33:1206-11.
20. Lee S, Pradhan B. Landslide hazard mapping at Selangor, Malaysia using frequency ratio and logistic regression models. Landslides; c2007. Available from: https://doi.org/10.1007/s10346-006-0047-y
21. Malczewski J. GIS and Multicriteria Decision Analysis and Multicriteria. Canada: John Wiley & Sons, Inc.; c1999.
22. Matin SS, Pradhan B. Challenges and limitations of earthquake-induced building damage mapping techniques using remote sensing images-A systematic review. Geocarto Int; c2021, 1-27. Available from: https://doi.org/10.1080/10106049.2021.1933213
23. Omarzadeh D, Karimzadeh S, Matsuoka M, Feizizadeh B. Earthquake aftermath from very high-resolution worldview-2 image and semi-automated object-based image analysis (Case study: Kermanshah, Sarpol-E Zahab, Iran). Remote Sensing. 2021;13:21. Available from: https://doi.org/10.3390/rs13214272
24. Ozdemir A, Altural T. A comparative study of frequency ratio, weights of evidence and logistic regression methods for landslide susceptibility mapping: Sultan Mountains, SW Turkey. J Asian Earth Sci. 2013;64:180-97. Available from: https://doi.org/10.1016/j.jseaes.2012.12.014
25. Park YJ, Kim BJ, Sung JHL. Appraisal of Drought Characteristics of Representative Drought Indices using Meteorological Variables. KSCE J Civil Eng. 2017;22(5):2002-2009. Available from: https://doi.org/10.1007/s12205-017-1744-x
26. Patel SK, Mathew B, Nanda A, Mohanty B, Saggurti N. Voices of rural people: Community-level assessment of effects and resilience to natural disasters in Odisha, India. Int J Popul Stud. 2020;6(1):3-15.
27. Pradhan B, Lee S, Buchroithner MF. Remote Sensing and GIS-based landslide susceptibility analysis and its cross-validation in three test areas using a frequency ratio model. Photogrammetrie Fernerkundung Geoinformation; c2010. Available from: https://doi.org/10.1127/1432-8364/2010/0037
28. Prasad AS, Pandey BW, Leimgruber W, Kunwar RM. Mountain hazard susceptibility and livelihood security in the upper catchment area of the river Beas, Kullu Valley, Himachal Pradesh, India. Geoenviron Disasters. 2016;3(1):3. Available from: https://doi.org/10.1186/s40677-016-0037-x
29. Rahmati O, Falah F, Dayal KS, Deo RC, Mohammadi F, Biggs T, *et al.* Machine learning approaches for spatial modeling of agricultural droughts in the south-east region of Queensland Australia. Sci Total Environ. 2020;699. Available from: https://doi.org/10.1016/j.scitotenv.2019.134230
30. Rahmati O, Falah F, Shaanu K, Deo RC, Mohammadi F, Biggs T, *et al.* Machine learning approaches for spatial modeling of agricultural droughts in the south-east region of Queensland Australia. Sci Total Environ. 2020;699:134230. Available from: https://doi.org/10.1016/j.scitotenv.2019.134230
31. Regmi NR, Giardino JR, Vitek JD. Modeling susceptibility to landslides using the weight of evidence approach: Western Colorado, USA. Geomorphology; c2010. Available from: https://doi.org/10.1016/j.geomorph.2009.10.002
32. Ripple WJ, Wolf C, Gregg JW, Levin K, Rockström J, Newsome TM, *et al.* World scientists' warning of a climate emergency 2022. Oxford University Press; c2022.
33. Rosselló J, Becken S, Gallego SM. The effects of natural disasters on international tourism: A global

analysis. Tourism Management. 2020;79:104080.
34. Rumpa NT, Real HRK, Razi MA. Disaster risk reduction in Bangladesh: A comparison of three major floods for assessing progress towards resilience. Int J Disaster Risk Reduct. 2023;97:104047.
35. Samanta S, Pal DK, Palsamanta B. Flood susceptibility analysis through remote sensing, GIS and frequency ratio model. Appl Water Sci. 2018. Available from: https://doi.org/10.1007/s13201-018-0710-1
36. Singh S, Kumar A, Negi MS. Hydro-morphological investigations of Neeru watershed using DEM and geospatial techniques. Int J Geography Geol Environ. 2022;4(2):13-23. Available from: https://doi.org/10.22271/27067483.2022.v4.i2a.110
37. Soltani A, Hewage K, Reza B, Sadiq R. Multiple stakeholders in multi-criteria decision-making in the context of municipal solid waste management: a review. Waste Management. 2015;35:318-328.
38. Susman P, O'Keefe P, Wisner B. Global disasters, a radical interpretation. In: Interpretations of calamity. Routledge; 2019. p. 263-283.
39. Tierney K. Disasters: A sociological approach. John Wiley & Sons; c2019.
40. Tirivarombo S, Osupile D, Eliasson P. Drought monitoring and analysis: standardised precipitation evapotranspiration index (SPEI) and Standardised Precipitation Index (SPI). Phys Chem Earth, Parts A/B/C. 2018;106:1s-10.
41. Tiwari A, Shoab M, Dixit A. GIS-based forest fire susceptibility modeling in Pauri Garhwal, India: a comparative assessment of frequency ratio, analytic hierarchy process and fuzzy modeling techniques. Nat Hazards. 2021;105(2):1189-1230. Available from: https://doi.org/10.1007/s11069-020-04351-8
42. Tran JB, Tran TD, Tran HTC. Monitoring drought vulnerability using multispectral indices observed from sequential remote sensing (Case Study: Tuy Phong, Binh Thuan, Vietnam). GIScience Remote Sensing. 2017;54(2):167-184. Available from: https://doi.org/10.1080/15481603.2017.1287838
43. Serrano VSM, Quiring SM, Gallardo PM, Yuan S, Castro DF. A review of environmental droughts: Increased risk under global warming? Earth-Sci Rev. 2020. Available from: https://doi.org/10.1016/J.EARSCIREV.2019.102953
44. Yagoub MM. Spatio-temporal and hazard mapping of Earthquake in UAE (1984-2012): Remote sensing and GIS application. Geoenviron Disasters. 2015;2(1):13. Available from: https://doi.org/10.1186/s40677-015-0020-y
45. Yalcin A, Reis S, Aydinoglu AC, Yomralioglu T. A GIS-based comparative study of frequency ratio, analytical hierarchy process, bivariate statistics and logistics regression methods for landslide susceptibility mapping in Trabzon, NE Turkey. Catena. 2011. Available from: https://doi.org/10.1016/j.catena.2011.01.014
46. Yao J, Zhao Y, Chen Y, Yu X, Zhang R. Multi-scale assessments of droughts: A case study in Xinjiang, China. Sci Total Environ. 2018;630:444-452. Available from: https://doi.org/10.1016/J.SCITOTENV.2018.02.200
47. Youssef AM, Pradhan B, Jebur MN, EHM. Landslide susceptibility mapping using ensemble bivariate and multivariate statistical models in Fayfa area, Saudi Arabia. Environ Earth Sci. 2015. Available from: https://doi.org/10.1007/s12665-014-3661-3